Elastic wavefield tomography with probabilistic petrophysical clustering

Odette Aragao & Paul Sava, Center for Wave Phenomena, Colorado School of Mines

SUMMARY

Full waveform inversion (FWI) aims to use all information provided by seismic data to deliver high resolution models of subsurface parameters. However, multiparameter FWI suffers from an inherent trade-off between parameters and from ill-posedness due to the highly nonlinear nature of FWI. Also, the models recovered using elastic FWI are subject to local minima if the initial models are far from the optimal solution. Moreover, an objective function purely based on the misfit between recorded and modeled data may honor the seismic data, but disregard the geological context. Hence, the inverted models may be geologically inconsistent, and thus not represent feasible lithological units. We propose that the aforementioned difficulties can be alleviated by explicitly incorporating petrophysical information into the inversion through a penalty function based on multiple probability density functions (PDFs), where each PDF represents a different lithology with distinct properties. We use K-means clustering to separate the petrophysical information into units of distinct lithologies are not easily distinguishable. Through synthetic examples, we demonstrate that the proposed framework leads FWI to elastic models that are superior to models obtained either without incorporating petrophysical information, or with a probabilistic penalty function based on a single PDF.

INTRODUCTION

The capability to deliver high resolution subsurface models has made full waveform inversion (FWI) a powerful tool for building models of seismic properties underlying wave propagation (Tarantola, 1984; Pratt, 1999; Sirgue and Pratt, 2004; Virieux and Operto, 2009). Conventionally, FWI functions as a data-fitting iterative procedure, i.e., it minimizes an objective function based on the misfit between recorded and simulated data, where the latter is modeled using a two-way wave equation in order to account for all wave propagation mechanisms. At each iteration, the considered wave equation employs the current subsurface model, which is updated by perturbations derived from the gradient of an objective function, usually computed using the adjoint state method (Plessix, 2006).

However, the inverse problem constrained by wave-equation presents many difficulties. FWI is ill-posed and highly nonlinear in relation to the model parameters (Symes, 2008). Moreover, if the initial subsurface models are not kinematically accurate to predict data with an error lower than the dominant wavelenght, the data residual suffers from cycle skipping and the inversion leads to models corresponding to local minima.

Compared to implementations using the isotropic acoustic wave equation (Tarantola, 1984; Pratt, 1990; Pratt et al., 1996), elastic FWI is more accurate in describing the physics of wave propagation in the earth (Tarantola, 1988; Pratt, 1990). An isotropic elastic wave equation can be written in terms of P- and S-wave velocities or Lamé parameters, λ and μ. However, the inverse problem is more ill-posed when estimating multiple parameters, due to the additional degrees of freedom in the model space (Operto et al., 2013). Moreover, different elastic properties may be coupled and updates of one parameter may leak into others, an effect known as crosstalk. In addition, the combinations of different components in the recovered model parameters can be lithologically implausible or impossible as model parameters are updated simultaneously, but independently.

One can reduce the number of possible solutions for ill-posed FWI by adding a model regularization term to the objective function, by using Tikhonov regularization (Tikhonov and Arsenin, 1977; Tarantola, 2005), total variation (Guitton, 2012; Zhang et al., 2019) or a prior model term (Tarantola, 2005; Asnaashari et al., 2013; Zhang et al., 2018) if additional geological information is available prior to the inversion. However, these techniques do not solve the problem of model updates that represent implausible lithologies. Moreover, as the model regularization terms operate in the spatial domain, they can guide inversion towards models that do not truly represent the subsurface, when accurate geological information about the entire studied region is not taken into account.

Petrophysical information provided by well logs describes the model only at sparse locations and therefore well log information cannot easily form the basis of model regularization in the space domain. As an alternative, one can apply petrophysical constraints in the model parameter space, in order to constrain the relationship between the model parameters during the inversion. This is the approach we take in this work. We use probabilistic model constraints, by explicitly using petrophysical information during the inversion in order to recover models that honor both geophysical and petrophysical data. We incorporate a penalty function, based on probability density functions (PDFs), into the FWI objective function. The petrophysical data are treated in the model parameter space, while the geophysical data are treated in the physical space.

One can use a single PDF to constrain the entire subsurface model. However, the available petrophysical information may indicate the occurrence of many lithological units. This indication can be evident, such that different lithologies are well defined in the petrophysical space, i.e., the PDF represents a multimodal distribution. Still, when building petrophysical PDFs from well log data, one may not be able to differentiate distinct lithological units because the range of elastic parameters for these lithologies overlap. In this case, we can use classification methods, such as K-means clustering (MacQueen, 1967), to categorize the petrophysical information into different units. We refer to a lithological unit as a *cluster*, representing a group of objects that have similar or correlated properties (Hartigan, 1975).

In order to recover subsurface models that represent different lithologies with distinct properties through constrained FWI, we propose to use petrophysical penalty terms based on different PDFs for each lithological unit, as derived from the available petrophysical information. Before this probabilistic

penalty term can be applied, we need to categorize each point of the updated model to the most representative cluster. For this purpose, we determine the distance from each point in the model to the center of the considered clusters, and then select the closest cluster for the petrophysical penalty.

We illustrate the performance of the proposed framework with two synthetic examples. We show the critical effect of the probabilistic penalty term when we use multiple PDFs compared to the cases of unconstrained FWI or of a single PDF used to describe the entire model.

THEORY

We use the isotropic elastic wave equation that assumes slowly varying Lamé parameters, such that their spatial gradients can be neglected,

$$\rho\ddot{\mathbf{u}} - \lambda[\nabla(\nabla\cdot\mathbf{u})] - \mu\left[\nabla\cdot\left(\nabla\mathbf{u}+\nabla\mathbf{u}^T\right)\right] = \mathbf{f}, \tag{1}$$

where $\mathbf{u}(e,\mathbf{x},t)$ is the elastic wavefield, $\mathbf{f}(e,\mathbf{x},t)$ is the source function, $\lambda(\mathbf{x})$ and $\mu(\mathbf{x})$ are the Lamé parameters, $\rho(\mathbf{x})$ is the density and e, $\mathbf{x}$ and t are, respectively, the experiment index, space coordinates and time.

The full waveform inverse problem is solved by minimizing an objective function $\mathcal{J}(\mathbf{u}_s,\lambda,\mu)$ consisting of a term that estimates the misfit between the predicted and observed data $\mathcal{J}_D(\mathbf{u}_s,\lambda,\mu)$; a model regularization term $\mathcal{J}_M(\lambda,\mu)$ that operates in the spatial domain and emphasize spatial correlation among the model parameters; and a term that applies probabilistic model constraints using a petrophysical penalty term, $\mathcal{J}_P(\lambda,\mu)$. Here, we do not use $\mathcal{J}_M(\lambda,\mu)$.

We can define the misfit term $\mathcal{J}_D(\mathbf{u}_s,\lambda,\mu)$ as

$$\mathcal{J}_D(\mathbf{u}_s,\lambda,\mu) = \sum_e \frac{1}{2}\left\|\mathbf{W}_u\mathbf{u}_s - \mathbf{d}_{obs}\right\|^2, \tag{2}$$

where $\mathbf{d}_{obs}(e,\mathbf{x},t)$ are the observed data and $\mathbf{W}_u(e,\mathbf{x},t)$ are weights that restrict the source wavefield $\mathbf{u}_s(e,\mathbf{x},t)$ to the receiver locations. We use a gradient-based method (Tarantola, 1988) to update the model, and compute the gradient of $\mathcal{J}_D$ with respect to λ and μ using the adjoint-state method (Plessix, 2006).

When one considers an objective function for the elastic FWI problem consisting of only $\mathcal{J}_D$, the components of the model parameters λ and μ are updated independently. Therefore, they can become physically inconsistent with each other, leading to an infeasible geologic representation of the subsurface. Alternatively, if we have access to petrophysical information obtained, e.g., from well logs, we can impose a penalty term that operate in the model parameter space.

We use a petrophysical penalty term $\mathcal{J}_P(\lambda,\mu)$, built using a probabilistic approach, into the objective function. From available well log data, we create a probability density function (PDF), whose cells of indices (i,j) represent the probability of occurance of the model components $(\lambda(i),\mu(j))$. For any given model with components $(\lambda_\mathbf{x},\mu_\mathbf{x})$ we evaluate in the model parameter space the distance to a point in the model space by

$$d_x(i,j) = \sqrt{[\lambda(i)-\lambda_\mathbf{x}]^2 + [\mu(j)-\mu_\mathbf{x}]^2}, \tag{3}$$

for $i = 1\cdots N_\lambda$ and $j = 1\cdots N_\mu$ where N_λ and N_μ are the numbers of discrete intervals defined for parameters λ and μ, respectively. We calculate a weighted distance from $(\lambda_\mathbf{x},\mu_\mathbf{x})$ to the whole PDF by using the probability of each cell $P(i,j)$:

$$D_\mathbf{x} = \sum_{i,j}\frac{P(i,j)}{d_x(i,j)}, \tag{4}$$

and then define the petrophysical penalty term $\mathcal{J}_P$ as

$$\mathcal{J}_P(\lambda,\mu) = \eta\sum_\mathbf{x}\frac{1}{D_\mathbf{x}}, \tag{5}$$

a where η is a scalar parameter that determines the strength of $\mathcal{J}_P(\lambda,\mu)$. By incorporating $\mathcal{J}_P(\lambda,\mu)$ into the FWI object function, the elastic parameters are linked during the inversion.

The occurance of many lithological units may be indicated by the available petrophysical information, with different lithologies well defined and isolated in the petrophysical space. In this case, one may not use a petrophysical penalty term based on a single PDF to represent the entire model, i.e., a single PDF to describe many lithologies. We propose to use a petrophysical penalty term based on multiple PDFs, each representing a different lithological unit. In order to do so, we categorize each given model with components $(\lambda_\mathbf{x},\mu_\mathbf{x})$ to a specific cluster, by calculating the distance between $(\lambda_\mathbf{x},\mu_\mathbf{x})$ and the center of each PDF. Then, we use the closest PDF to build the petrophysical penalty related to $(\lambda_\mathbf{x},\mu_\mathbf{x})$.

Nevertheless, the occurance of different lithologies may not be evident in the available petrophysical data. In this case, one may not be able to differentiate distinct lithological units in the PDF. One solution is to apply K-means clustering to separate the petrophysical information into different PDFs, where each PDF represents a lithological unit. K-means clustering consists of five steps (MacQueen, 1967; Hartigan, 1975): 1- define the number of clusters k; 2- initiate the algorithm with randomly selected center for each cluster; 3- assign each point of the available petrophysical data to the closest center; 4- update the center of each cluster as the mean of the points that were assigned to that cluster; 5- repeat steps 3 and 4 until no points are re-assigned, i.e., there is no change in center values. After defining the clusters, we build a different PDF for each cluster and then follow the same approach as discussed above.

EXAMPLES

The synthetic examples use a portion of the Marmousi 2 model (Martin et al., 2002). For the first example, different lithologies are well defined and isolated in the petrophysical space. We aim to show how the probabilistic penalty term based on multiple PDFs guides the inversion toward more accurate models compared to the cases of unconstrained FWI or of FWI using a probabilistic penalty term based on a single PDF. In the second example, we use a different correct model, where the available petrophysical information do not indicate the occurrence of separate lithological units. We use the K-means clustering technique to categorize the petrophysical information into clusters and to create different PDFs for the petrophysical penalty term.

Clustered Marmousi 2 model

For the first example, we modify the model to represent well-defined and distinct lithologies. We consider that prior petrophysical data from three well logs are available and we use this information to build the petrophysical model penalty. Figure 1 shows the correct λ and μ models, the well locations

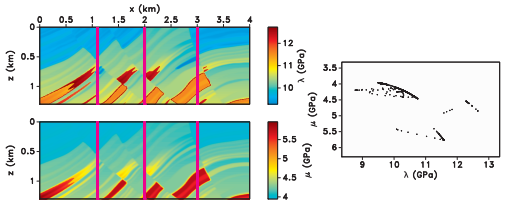

Figure 1: Clustered Marmousi 2 model: true λ and μ models. The vertical lines correspond to well locations that provide the data shown in the crossplot.

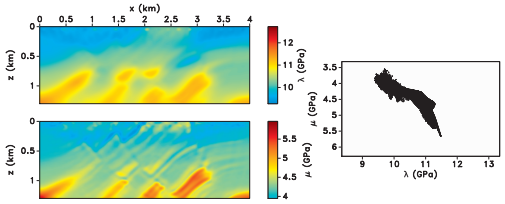

Figure 2: Recovered λ and μ models obtained using the objective function $\mathcal{J}_D$ for the clustered Marmousi model.

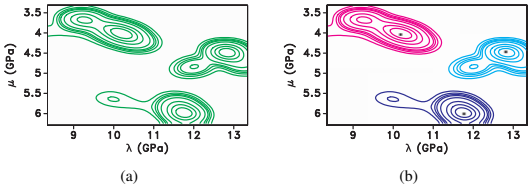

Figure 3: (a) PDF associated with the term $\mathcal{J}_{P1}$ and (b) PDF associated with the term $\mathcal{J}_{P2}$. We estimate the PDFs in (a) and (b) from the well logs shown in Figure 1.

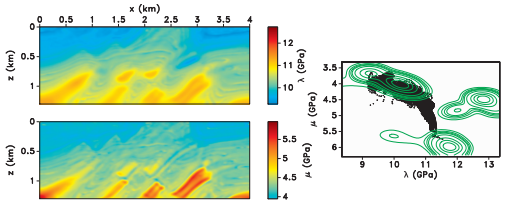

Figure 4: Recovered λ and μ models using the objective function $\mathcal{J}_D + \mathcal{J}_{P1}$ for the clustered Marmousi model. The green contours overlain on the crossplot illustrate the probabilistic penalty term based on a single PDF $\mathcal{J}_{P1}$.

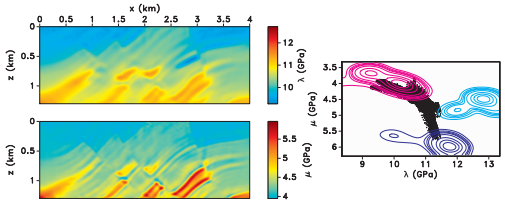

Figure 5: Recovered λ and μ models using the objective function $\mathcal{J}_D + \mathcal{J}_{P2}$for the clustered Marmousi model. The contours with different colors overlain on the crossplot illustrate multiple PDFs used in the probabilistic penalty $\mathcal{J}_{P2}$.

and the model parameters crossplot and the crossplot of λ and μ models extracted at the wells located at $x = 1.1$, 2.0 and 3.0 km, which indicates the presence of three separate lithological units (Figure 1). For this example, we obtain initial models by smoothing the true model.

Figure 2 shows the recovered λ and μ models using the objective function $\mathcal{J}_D$. As we do not include petrophysical information during inversion, the μ model shows spurious artifacts due to the trade-off with the elastic parameters. The recovered μ model also has more structural detail than the recovered λ model, as the S-wave wavelenght is shorter than that of P waves. Additionally, the amplitude of the low velocity anomaly presented in the true λ model (Figure 1) at $x = 3$ km and $z = 0.5$ km is not well recovered during the inversion.

For this example, in order to perform the inversion using the petrophysical penalty term, we carry out two tests. For the first test, we use a single PDF to constrain the entire model, even though the crossplot of λ and μ provided by the well logs (Figure 1) indicates well defined separate lithologies. The first test uses the objective function $\mathcal{J}_D + \mathcal{J}_{P1}$. Figure 3a shows the single PDF used in $\mathcal{J}_{P1}$, which corresponds to three clusters. For the second test, we use different PDFs to constrain the model, and the objective function uses $\mathcal{J}_D$ and $\mathcal{J}_{P2}$. Figure 3b shows the different PDFs used in $\mathcal{J}_{P2}$. The black dot inside each PDF in Figure 3b represents the center of the PDF and we use these points to decide which PDF is used to constrain each point in the model, i.e., decide to which cluster each point of the updated model is more likely to represent.

Figure 4 shows the recovered λ and μ models using the objective function $\mathcal{J}_D + \mathcal{J}_{P1}$. Different from the unconstrained inversion (Figure 2), the recovered λ and μ models have similar spatial resolution. Additionally, the inversion is able to recover the amplitude of the low velocity anomaly present in the true λ model (Figure 1) at $x = 3$ km and $z = 0.5$ km better than the inversion using the objective function $\mathcal{J}_D$ (Figure 2). However, the inverted models depicted in Figure 4 are noisy and do not show blocky structures as in the true models (Figure 1). In addition, the crossplot shown in Figure 4 shows that the inversion could not recover model with $\lambda > 11.5$ GPa and $4.0 < \mu < 5.0$ GPa. Also, the majority of the points in the crossplot of Figure 4 are inside the distribution with $\lambda < 11.0$ GPa and $\mu < 4.5$ GPa. Therefore, when petrophysical information indicates the presence of distinct lithologies, but we choose to use a penalty term based on a single PDF for the entire model, the cluster with larger probability attracts most model points during the inversion.

Figure 5 shows the recovered λ and μ models using the objective function $\mathcal{J}_D + \mathcal{J}_{P2}$. The contours correspond to three PDFs, each representing a cluster. The inverted λ and μ models shown in Figure 5 have comparable resolution and are closer to the true models compared with the cases when we use the objective functions $\mathcal{J}_D$ (Figure 2) or $\mathcal{J}_D + \mathcal{J}_{P1}$ (Figure 4). Additionally, the artifacts in the μ model caused by interparameter crosstalk are reduced. Notice that the crossplot built with the inverted models (Figure 5) shows points inside all three PDFs.

Marmousi 2 model with clustering

For the second example, we use a different correct model,

where the available petrophysical information do not indicate the occurrence well-defined and distinct lithologies. Figure 6 shows the correct λ and μ models, the well locations and the model parameters crossplot and the crossplot of λ and μ models extracted at the wells located at $x = 1.1$, 2.0 and 3.0 km. Once again, we obtain initial models by smoothing the true model for this experiment.

Figure 7 shows the recovered λ and μ models using the objective function $\mathcal{J}_D$. Once again, one can notice that the inverted μ model has higher spatial resolution. Also, the μ model has spurious artifacts due to parameter crosstalk.

The crossplot shown in Figure 6 does not describe distinct lithologies. Therefore, one can choose to use a single PDF (Figure 8a) to constrain the entire model and using the objective function $\mathcal{J}_D + \mathcal{J}_{P1}$. However, we use K-means clustering to separate the petrophysical information in the crossplot depicted in Figure 6 into multiple PDFs and then employ the objective function $\mathcal{J}_D + \mathcal{J}_{P2}$. For this example, we define four clusters (Figure 8b).

Figure 9 shows the recovered λ and μ models using the objective function $\mathcal{J}_D + \mathcal{J}_{P1}$. Both λ and μ models have similar resolution and are better recovered compared with the cases when we use the objective functions $\mathcal{J}_D$ (Figure 7). Additionally, the μ model artifacts caused by interparameter crosstalk are attenuated. However, the inverted λ model depicted in Figure 9 is noisy and does not show blocky structures above $x = 1.0$ km.

Figure 10 shows the recovered λ and μ models using the objective function $\mathcal{J}_D + \mathcal{J}_{P2}$. Both λ and μ inverted models depicted in Figure 10 show high resolution and are closer to the true models compared with the cases when we use the objective functions $\mathcal{J}_D$ (Figure 7) or $\mathcal{J}_D + \mathcal{J}_{P1}$ (Figure 9). The μ model shown in Figure 10 shows reduced crosstalk, and the λ model has blocky structure that conform to the true models (Figure 6).

CONCLUSIONS

We develop a strategy for incorporating petrophysical information into elastic full waveform inversion through a penalty term based on multiple probability density functions. We demonstrate that imposing this kind of penalty improves the quality of the recovered subsurface models and better represents feasible lithologies. Through two synthetic examples, we verify the effectiveness of the proposed method in leading inversion towards the true models. We also show that the quality of the recovered models can be compromised when the penalty function is based on a single probability density function, while petrophysical information indicates the occurrence of different lithologies in the subsurface. We demonstrate that K-means clustering can be used to separate the petrophysical data into different lithological units in order to compute multiple separate probability density functions.

ACKNOWLEDGMENTS

We acknowledge CAPES (Brazilian Federal Agency for Support and Evaluation of Graduate Education) for financial support. We thank the sponsors of the Center for Wave Phenomena (CWP), whose support made this research possible. The synthetic examples in this paper uses the Madagascar open-source software package (Fomel et al., 2013) freely available from http://www.ahay.org.

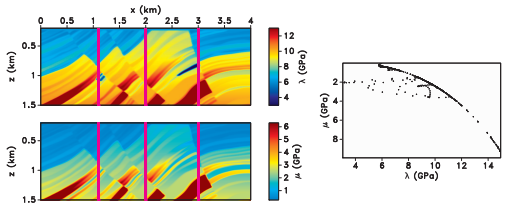

Figure 6: True λ and μ models and their crossplot for the inversion with clustering. The vertical lines correspond to well locations that provide the data shown in the crossplot.

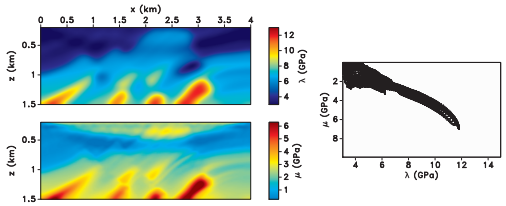

Figure 7: Recovered λ and μ models obtained using the objective function $\mathcal{J}_D$ for the inversion with clustering.

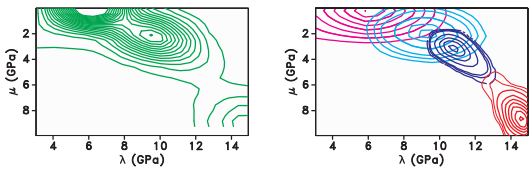

Figure 8: (a) PDF associated with the term $\mathcal{J}_{P1}$ and (b) PDF associated with the term $\mathcal{J}_{P2}$. We estimate the PDFs in (a) and (b) from the well logs shown in Figure 6.

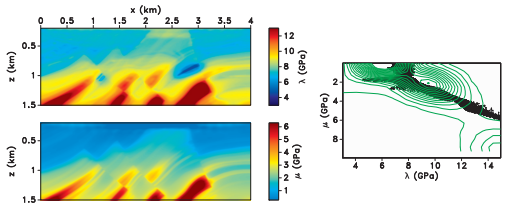

Figure 9: Recovered λ and μ models using the objective function $\mathcal{J}_D + \mathcal{J}_{P1}$ for the inversion with clustering.

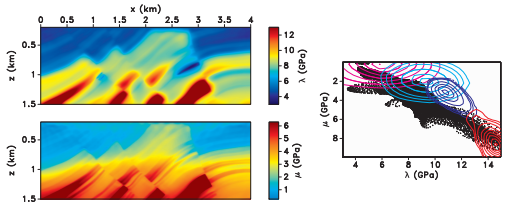

Figure 10: Recovered λ and μ models using the objective function $\mathcal{J}_D + \mathcal{J}_{P2}$ for the inversion with clustering.

REFERENCES

Asnaashari, A., R. Brossier, S. Garambois, F. Audebert, P. Thore, and J. Virieux, 2013, Regularized seismic full waveform inversion with prior model information: Geophysics, **78**, R25–R36.

Fomel, S., P. Sava, I. Vlad, Y. Liu, and V. Bashkardin, 2013, Madagascar: open-source software project for multidimensional data analysis and reproducible computational experiments: Journal of Open Research Software, 8th ed., DOI: http://dx.doi.org/10.5334/jors.ag.

Guitton, A., 2012, Blocky regularization schemes for full-waveform inversion: Geophysical Prospecting, **60**, 870–884.

Hartigan, J. A., 1975, Clustering algorithms: John Wiley & Sons.

MacQueen, J. B., 1967, Some methods for classification and analysis of multivariate observations: Presented at the 5th Berkeley Symposium on Mathematical Statistics and Probability.

Martin, G., K. Marfut, and S. Larsen, 2002, Marmousi-2, an updated model for the investigation of avo in structurally complex areas: Presented at the SEG Technical Program Expanded Abstracts.

Operto, S., Y. Gholami, V. Prieux, A. Ribodetti, R. Brossier, L. Metivier, and J. Virieux, 2013, A guided tour of multiparameter full-waveform inversion with multicomponent data: from theory to practice: The Leading Edge, **32**, no. 9, 1040–1054.

Plessix, R. E., 2006, A review of the adjoint-state method for computing the gradient of a functional with geophysical applications: Geophysical Journal International, **167**, no. 2, 495–503.

Pratt, R. G., 1990, Inverse theory applied to multi-source cross-hole tomography: Geophysical Prospecting, **38**, 311–329.

———, 1999, Seismic waveform inversion in the frequency domain. Part 1: Theory and verification in a physical scale model: Geophysics, **64**, 888–901.

Pratt, R. G., Z. M. Williamson, and M. Warner, 1996, Two-dimensional velocity model from wide-angle seismic data by wavefield inversion: Geophysical Journal International, **124**, 323–340.

Sirgue, L., and R. Pratt, 2004, Efficient waveform inversion and imaging: a strategy for selecting temporal frequencies: Geophysics, **69**, 231–248.

Symes, W. W., 2008, Migration velocity analysis and waveform inversion: Geophysical Prospecting, **56**, no. 6, 765–790.

Tarantola, A., 1984, Inversion of seismic reflection data in the acoustic approximation: Geophysics, **49**, 1259–1266.

———, 1988, Theoretical background for the inversion of seismic waveforms including elasticity and attenuation: Pure and Applied Geophysics, **128**, 365–399.

———, 2005, Inverse Problem Theory and Methods for Model Parameter Estimation: Society for Industrial and Applied Mathematics.

Tikhonov, A., and V. Arsenin, 1977, Solution of ill-posed problems: Winston and Sons.

Virieux, J., and S. Operto, 2009, An overview of full-waveform inversion in exploration geophysics: Geophysics, **74**, no. 6, WCC1–WCC26.

Zhang, Z., T. Alkhalifah, E. Z. Naeini, and B. Sun, 2018, multiparameter elastic full waveform inversion with facies-based constraints: Geophysical Journal International, **213**, 2112–2127.

Zhang, Z., T. Alkhalifah, Z. Wu, Y. Liu, B. He, and J. Oh, 2019, Normalized nonzero-lag crosscorrelation elastic full-waveform inversion: Geophysics, **84**, no. 1, R1–R9.